

Petschek-like reconnection with uniform resistivity

H. Baty,^{1,a)} E. R. Priest,^{2,b)} and T. G. Forbes^{3,c)}

¹*Observatoire Astronomique de Strasbourg, 11, Rue de l'Université, 67000 Strasbourg, France*

²*Institute of Mathematics, University of St. Andrews, Fife KY169SS, Scotland, United Kingdom*

³*Institute for the Study of Earth, Oceans, and Space, University of New Hampshire, Durham, New Hampshire 03824, USA*

(Received 8 April 2009; accepted 22 May 2009; published online 15 June 2009)

Using two-dimensional time dependent viscoresistive magnetohydrodynamic simulations, we report for the first time the existence of fast stationary magnetic reconnection with a spatially uniform plasma resistivity. This is achieved through the use of a nonuniform well tailored viscosity profile, following requirements deduced by Baty *et al.* [Phys. Plasmas **16**, 012102 (2009)]. The quasisteady state exhibits the global features of a classical Petschek solution, with two pairs of standing slow-mode shocks attached to a central diffusion region and a fast-mode expansion of the inflowing plasma. The diffusion region is however influenced by the viscosity with a two-component structure, and the reconnection rate is observed to be slightly higher than nonviscous nonuniform resistive reconnection. © 2009 American Institute of Physics. [DOI: [10.1063/1.3155087](https://doi.org/10.1063/1.3155087)]

Magnetic field reconnection plays a fundamental role for the dynamics of astrophysical and laboratory plasmas. It allows a change in field topology, resulting in the conversion of magnetic energy into heating and acceleration of plasma. For collisional media such as the low solar atmosphere and tokamak plasmas, the magnetohydrodynamic (MHD) approach is relevant. Two-dimensional (2D) MHD reconnection can now be said to be fairly well understood. The more recent studies are focusing on three-dimensional aspects,¹ and on collisionless and Hall MHD effects.²

However, there is one controversial aspect that even now remains puzzling. It concerns the existence of the fast reconnection regime called Petschek's mechanism.³ Numerical MHD simulations have failed to obtain a Petschek-like solution when they use a spatially uniform resistivity. In contrast, Petschek reconnection can be produced when a nonuniform resistivity enhanced at the X-point of the central diffusion region is adopted.^{4–7} In the original model of Petschek, no assumption was made about the spatial dependence of the resistivity, and so this led to the suggestion that the Petschek model may be incorrect for a uniform resistivity (see Ref. 8 and references therein, and Ref. 9). This point is not purely academic since the answer could be of great importance for understanding general aspects of magnetic reconnection in two and three dimensions as well. Furthermore, in contrast to slow Sweet–Parker reconnection,^{10,11} fast reconnection rates as allowed by Petschek's mechanism are needed to explain the rapid release of magnetic energy which occurs in phenomena such as solar flares and tokamak disruptions.

In a previous paper (referenced as paper 1 below),¹² we have explored the effect of using a nonlocalized resistivity. Indeed, we have shown that it is possible to obtain Petschek-like reconnection in a half plane where a uniform resistivity is imposed. This is helped by a Petschek solution produced

in the other half plane where a classical decreasing resistivity profile is adopted. In this way, a uniform resistivity solution appears to be driven and maintained by a coexisting nonuniform resistivity Petschek configuration. The configuration is asymmetric, with a stagnation point flow (located in the uniform resistivity half plane) which does not coincide with the X-point. The latter result suggests a potential way to decouple the two points by employing a specific well tailored viscosity profile in a viscoresistive model. In a real plasma, there is no reason to neglect the viscosity (as assumed in most previous MHD simulations). This neglect is even surprising, as in typical coronal plasmas the bulk viscosity Reynolds number is believed to be many orders of magnitude smaller than the magnetic Reynolds number.¹³ The work that we present here is precisely devoted to this point.

The setup of the experiments follows previous papers, in which one assumes initially a classical Harris current sheet configuration, with a magnetic field parallel to the y axis and varying with x ,

$$\mathbf{B} = B_e \tanh(x/a)\mathbf{y}, \quad (1)$$

where B_e is the amplitude of the field and a is the initial half width of the current sheet. A static equilibrium with an isothermal medium is considered. We set $B_e=1$ and $a=0.1$ to define our normalization. A rather moderate value at the boundary $x=\pm L_x$ of the plasma β is also chosen, namely, $\beta=0.35$. The initial plasma pressure and density are then set to be $p(x)=0.675-B_y^2/2$ and $\rho(x)=2p(x)/\beta$, respectively. We solve the full set of nonlinear MHD viscoresistive equations as an initial value problem, in two spatial dimensions and Cartesian geometry (x,y) . The equations are the same as in Ref. 6 except for the addition of a shear viscosity (a simplified stress tensor with zero bulk viscosity is adopted, following Eqs. 1.3 and 1.5 given by Priest and Forbes¹). A total of 400×200 spatial grid points is used in the spatial domain $-L_x \leq x \leq L_x$ and $-L_y \leq y \leq L_y$ of dimensions $L_x=1$ and $L_y=2$. A nonuniform spacing with a grid accumulation is chosen in order to have sufficient cells to resolve the central

^{a)}Electronic mail: baty@astro.u-strasbg.fr.

^{b)}Electronic mail: eric@mcs.st-and.ac.uk.

^{c)}Electronic mail: terry.forbes@unh.edu.

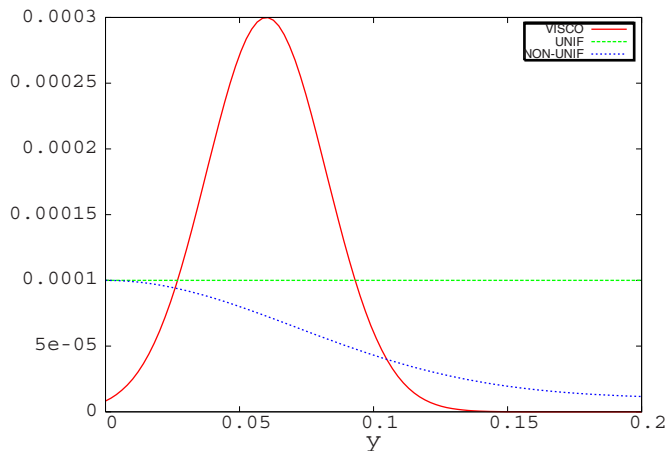


FIG. 1. (Color online) Profile of the viscosity as a function of y as a plain line (visco). Also shown are the resistivity variations when the resistivity is nonuniform (nonunif) as a dotted line, and uniform (unif) as a dashed line.

current sheet. Typically, we are able to achieve a minimum grid spacing of $\Delta x = 7 \times 10^{-4}$ and $\Delta y = 5 \times 10^{-3}$ in the x and y directions, respectively. The boundary conditions are imposed through the use of two ghost cells situated slightly outside the computational domain at each boundary. Following paper 1, a procedure with overspecified boundary conditions at the inflow boundary $x = \pm L_x$ is used. Additionally, free conditions are also imposed at the outflow boundaries $y = \pm L_y$ (see also Ref. 14). We use the general finite-volume based Versatile Advection Code (VAC),¹⁵ and select the explicit one-step total variation diminishing scheme with minmod limiting.^{16,17} This is a second-order accurate shock-capturing method making use of a Roe-type approximate Riemann solver. To handle the solenoidal constraint on the magnetic field $\nabla \cdot \mathbf{B} = 0$, our VAC simulations apply a projection scheme at every time step, in order to remove any numerically generated divergence of the magnetic field up to a predefined level close to the machine accuracy.^{18,19}

A two-step procedure has been used in this work. Indeed, in order to build up a reconnection solution forming an X-point topology, it is necessary to use an enhanced resistivity at the domain center in a first stage. We therefore adopt $\eta(x, y) = (\eta_0 - \eta_1) \exp[-(x/l_x)^2 - (y/l_y)^2] + \eta_1$, where η_0 and η_1 are the normalized resistivities at the center of the domain and of the background region, respectively. The resistivity coefficient η is connected with the magnetic Reynolds number R_{me} via $R_{me} = 2/\eta$. l_x and l_y are the characteristic length scales of the resistivity variation. We use $\eta_0 = 10^{-4}$ and $\eta_1 = 1 \times 10^{-5}$, and $l_x = 0.05$ and $l_y = 0.1$. At the same time, a viscosity profile $\nu(x, y) = \nu_0 \exp[-(x/l_x)^2 - (|y| - 0.06)^2 / 0.001]$ is taken, whose variation with y is plotted in Fig. 1. This nonmonotonic variation along the y direction is tailored in order to slow down the plasma outflow (ejected from the X-point) over a length comparable to the characteristic resistive length l_y . Indeed, we follow the idea developed in paper I, with the aim of trying to decouple the X-point and the stagnation point flow. Note that the maximum normalized viscosity is $\nu_0 = 3 \times 10^{-4}$.

Once a steady-state reconnection is obtained (such that the time variation of the electric field at the X-point is less

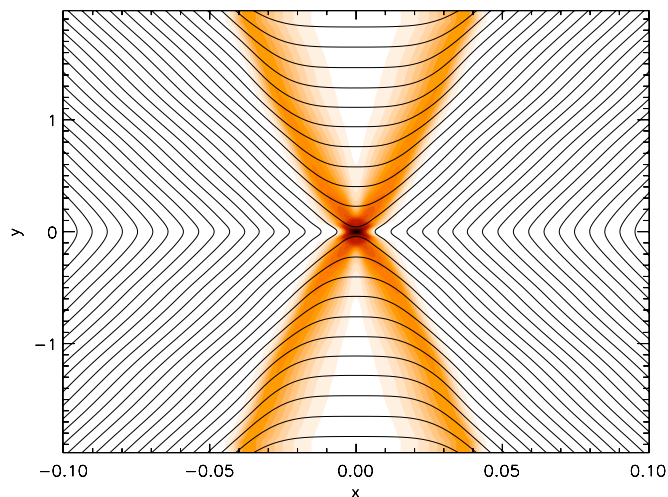


FIG. 2. (Color online) Magnetic field lines and current density structures obtained for the viscous (VISC) steady-state configuration, using a uniform resistivity $\eta = 10^{-4}$ and maximum viscosity $\nu_0 = 3 \times 10^{-4}$.

than 1%–2%), a uniform resistivity $\eta(x, y) = \eta_0$ is then imposed to pursue the simulation (the viscosity profile remaining unchanged) in the second step. A new steady-state solution (VISC) is subsequently obtained at the end of this second stage. The magnetic field and associated current density obtained in this way are very similar to a classical Petschek solution using a nonuniform resistivity and zero viscosity (REF), as one can see in Figs. 2 and 3. Indeed, one can clearly see that in both cases two pairs of standing slow-mode shocks emanate from the corners of a small central diffusion region. Note that the shocks are thicker for the uniform resistivity case due to the higher level of diffusion in the background region.

However, there are a number of noticeable differences that are listed below. First, a zoom on Figs. 2 and 3, as shown in Figs. 4 and 5, reveals that the geometry of the diffusion region is not similar. This is not surprising as a nonzero viscosity is expected to influence the dissipative re-

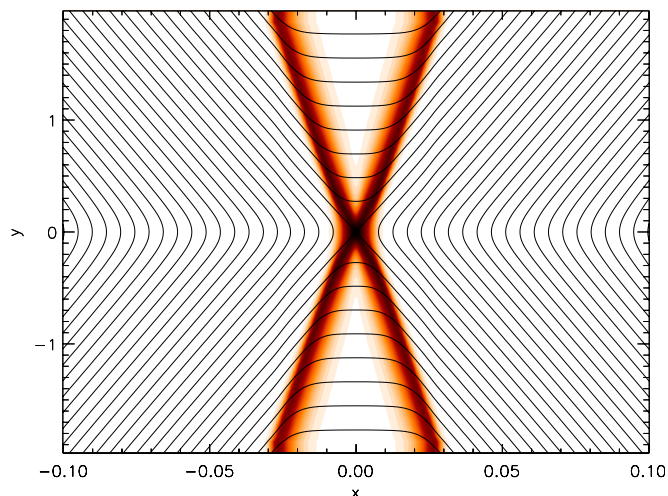


FIG. 3. (Color online) Same as in Fig. 2 for the reference (REF) steady-state configuration, using a nonuniform resistivity (the maximum resistivity is $\eta_0 = 10^{-4}$ at the X-point) and zero viscosity.

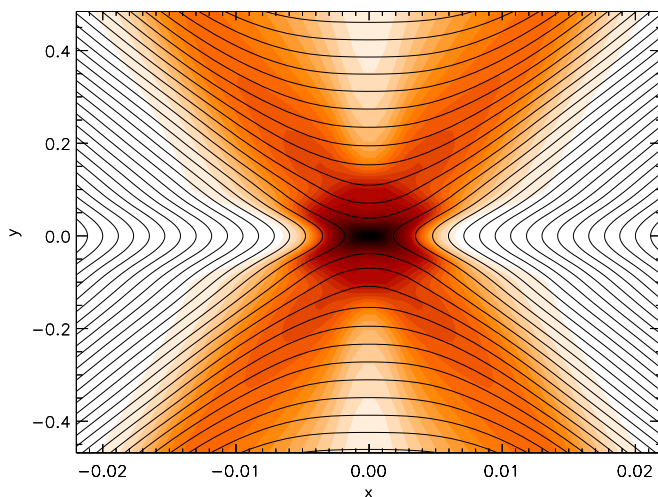


FIG. 4. (Color online) Zoom of Fig. 2.

gion leading to a viscoresistive layer with a characteristic length scale $(\eta\nu)^{1/4}$, which dominates over the pure resistive scale in $\eta^{1/2}$ when $\eta < \nu$.²⁰ In our VISC solution, we observe that the diffusion layer has a two-scale structure. Indeed, an inner resistive region having a classical rectangular shape appears to be surrounded by an outer viscoresistive region with an elongated non regular form (see Fig. 4), to which the shocks are attached. This two-component diffusion region is also in agreement with the current density structure plotted in Fig. 6. We have checked that the change in current slope coincides with the transition between the two components of the diffusion layer. As deduced from the outflow velocity structure plotted in Fig. 7, the stagnation point flow does not appear to be decoupled from the X-point. However, a two-scale structure is again present in the VISC run compared to the REF case, which constitutes the key ingredient to produce our uniform resistivity Petschek-like reconnection.

It is also instructive to investigate the transverse structure of the configuration. Indeed, as one can see in Fig. 8, the VISC solution exhibits the features of a fast-mode expansion expected from a classical Petschek solution. That is, when

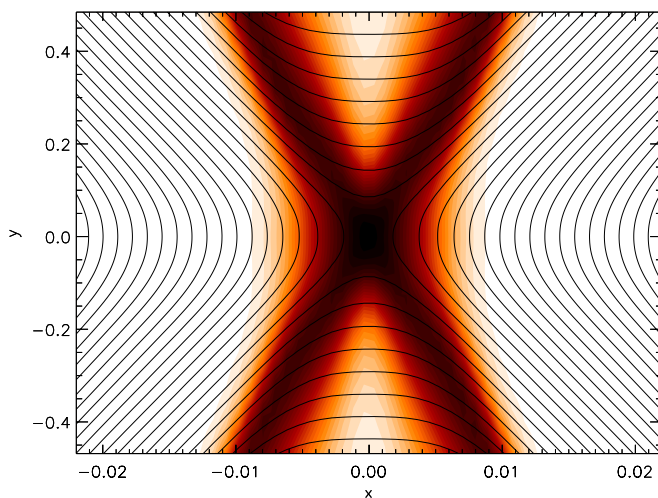
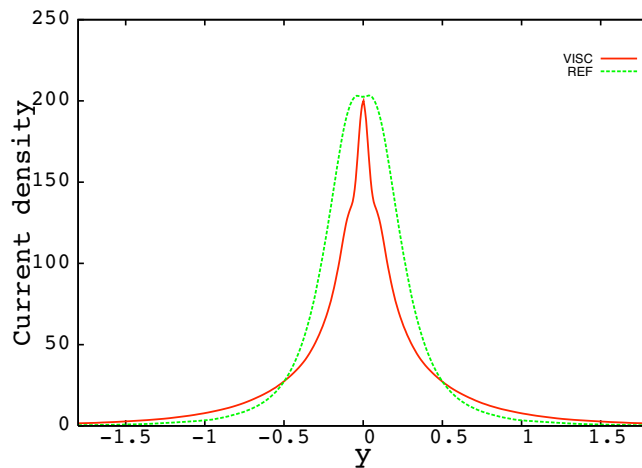


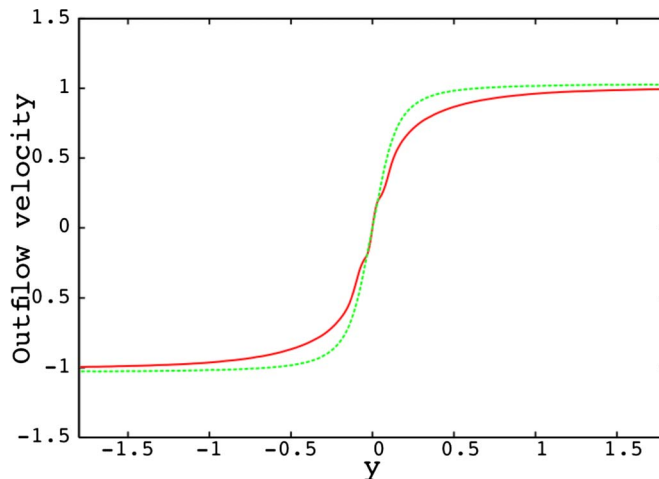
FIG. 5. (Color online) Zoom of Fig. 3.

FIG. 6. (Color online) Current density as a function of y for the uniform resistivity run (VISC) and classical non viscous nonuniform resistivity run (REF).

approaching the diffusion region from the inflow boundary, the magnetic field and thermal pressure are decreasing (only very slightly for the later) together. However, a slow-mode compression of weak amplitude and localized just front off the diffusion region is superposed on the whole variation. This later effect is a weak local flux-pileup effect, which results from the geometry of the viscoresistive layer and leads to the additional curvature of the magnetic field lines observed in Fig. 4.

Finally, we have measured the reconnection rate of the VISC solution, leading to a value of $M_e=0.027$ for the external Alfvén Mach number. The latter value is slightly higher than obtained for the REF case where $M_e=0.023$. However, it remains lower than the value expected from the maximum rate given by Petschek's famous formula $M_e = \pi / (8 \ln R_{me})$ (where R_{me} is the magnetic Reynolds number equal to 2×10^4 in our case), as $M_e=0.0396$.

We conclude that it is possible to obtain Petschek-like reconnection with a uniform resistivity in a viscous MHD

FIG. 7. (Color online) Outflow velocity as a function of y for the uniform resistivity run VISC (plain line) and classical nonviscous nonuniform resistivity run REF (dashed line).

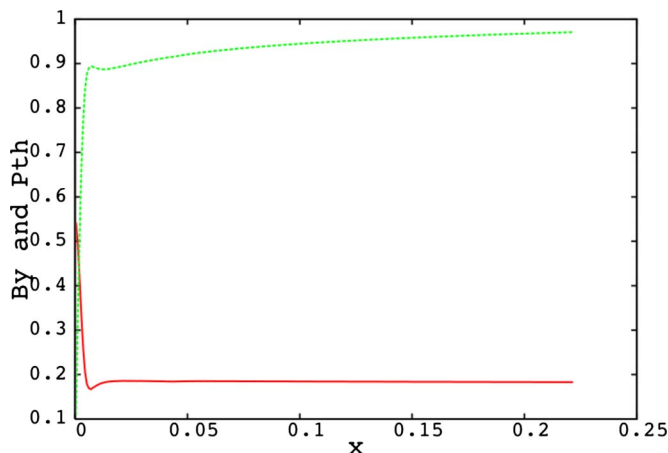


FIG. 8. (Color online) Thermal pressure $P(x)$ (plain line) and longitudinal magnetic field $B_y(x)$ (dashed line) dependences, obtained doing a $y=0$ cut for the VISC run.

model. A steady-state reconnection is produced through the use of a nonuniform viscosity having a well tailored profile in the longitudinal direction. A short analysis shows that our viscoresistive solution exhibits the global features of a classical Petschek reconnection. However, the central diffusion layer appears to have two-scale components with an inner resistive area surrounded by a more complicated viscoresistive region to which the shocks are attached. A reconnection rate is obtained that is slightly higher than with a classical nonuniform resistivity solution. Further studies of viscous magnetic reconnection including a parametric study (for the viscosity and resistivity profiles) are necessary in order to explore more deeply this subject, and also to connect our *ad hoc* profiles to a realistic physical context and perhaps adopting in future a more realistic viscous stress tensor.²¹ Despite some previous attempts to investigate some particular aspects of viscoresistive reconnection (see, for example, Refs. 20 and 22), our results clearly indicate the necessity for a modified model of the classical view of 2D steady-state reconnection solutions including the effect of viscosity. It

could also be of interest to compare how the present results modify the general view of magnetic reconnection when considering the other models (kinetic and fluid-based Hall models).

E. R. Priest is grateful to the UK Particle Physics and Astronomy Research Council and to the EU Solaire network for financial support. The contribution of T. G. Forbes was supported by the NSF under Grant Nos. ATM-0734032 and ATM-0752257, and NASA under Grant Nos. NNX08AG44G and NNX-06AC19G.

¹E. R. Priest and T. G. Forbes, *Magnetic Reconnection* (Cambridge University Press, Cambridge, 2000).

²J. F. Drake and M. A. Shay, in *Reconnection of Magnetic Fields: Magnetohydrodynamics and Collisionless Theory and Observations*, edited by J. Birn and E. R. Priest (Cambridge University Press, Cambridge, 2007), Chap. 3, p. 87.

³H. E. Petschek, *AAS-NASA Symposium on the Physics of Solar Flares*, edited by W. N. Hess (National Aeronautics and Space Administration, Washington, D.C., 1964), Vol. SP-50, p. 425.

⁴M. Ugai and T. Tsuda, *J. Plasma Phys.* **22**, 1 (1979).

⁵M. Ugai, *Plasma Phys. Controlled Fusion* **26**, 1549 (1984).

⁶M. Scholer, *J. Geophys. Res.* **94**, 8805, DOI: 10.1029/JA094iA07p08805 (1989).

⁷M. Yan, L. C. Lee, and E. R. Priest, *J. Geophys. Res.* **97**, 8277, DOI: 10.1029/92JA00170 (1992).

⁸R. M. Kulsrud, *Earth, Planets Space* **53**, 417 (2001).

⁹D. Biskamp, *Nonlinear Magnetohydrodynamics* (Cambridge University Press, Cambridge, 1993).

¹⁰P. A. Sweet, in *Electromagnetic Phenomena in Cosmic Physics*, edited by B. Lehnert (Cambridge University Press, Cambridge, 1958), p. 123.

¹¹E. N. Parker, *J. Geophys. Res.* **62**, 509, DOI: 10.1029/JZ062i004p00509 (1957).

¹²H. Baty, T. G. Forbes, and E. R. Priest, *Phys. Plasmas* **16**, 012102 (2009).

¹³J. V. Hollweg, *Astrophys. J.* **306**, 730 (1986).

¹⁴H. Baty, E. R. Priest, and T. G. Forbes, *Phys. Plasmas* **13**, 022312 (2006).

¹⁵G. Tóth, *Astrophys. Lett. Commun.* **34**, 245 (1996).

¹⁶P. Colella and P. R. Woodward, *J. Comput. Phys.* **54**, 174 (1984).

¹⁷A. Harten, *J. Comput. Phys.* **49**, 357 (1983).

¹⁸R. B. Brackbill and D. C. Barnes, *J. Comput. Phys.* **35**, 426 (1980).

¹⁹G. Tóth, *J. Comput. Phys.* **161**, 605 (2000).

²⁰I. J. D. Craig, Y. E. Litvinenko, and T. Senanayake, *Astron. Astrophys.* **433**, 1139 (2005).

²¹I. J. D. Craig and Y. E. Litvinenko, *Astrophys. J.* **667**, 1235 (2007).

²²Y. E. Litvinenko, *Phys. Plasmas* **13**, 092305 (2006).